Effect of temperature variations on equilibrium distances in levitating parallel dielectric plates interacting through Casimir forces

Victoria Esteso,[1] Sol Carretero-Palacios,[1, a)] and Hernán Míguez[1, b)]
Multifunctional Optical Materials Group, Instituto de Ciencia de Materiales de Sevilla (Consejo Superior de Investigaciones Científicas - Universidad de Sevilla), Calle Américo Vespucio 49, 41092 Sevilla, Spain

We study at thermal equilibrium the effect of temperature deviations around room temperature on the equilibrium distance (d_{eq}) at which thin films made of Teflon, silica or polystyrene immersed in glycerol levitate over a silicon substrate due to the balance of Casimir, gravity, and buoyancy forces. We find that the equilibrium nature (stable or unstable) of d_{eq} is preserved under temperature changes, and provide simple rules to predict whether the new equilibrium position will occur closer or further from the substrate at the new temperature. These rules depend on the static permittivities of all materials comprised in the system ($\varepsilon_0^{(m)}$) and the equilibrium nature of d_{eq}. Our designed dielectric configuration is excellent for experimental observation of thermal effects on the Casimir force indirectly detected through the tunable equilibrium distances (with slab thickness and material properties) in levitation mode.

I. INTRODUCTION

After the Casimir force was first predicted by H. Casimir as an attractive force between two ideal metallic plates at zero temperature due to vacuum fluctuations[1], one of the most striking results that followed was the prediction by E. Lifshitz of a repulsive force arising between bodies of arbitrary shape and dissimilar optical properties separated by a fluid medium at any temperature[2,3]. Since then, numerous studies considering different geometries and materials have been performed with the aim of controlling the repulsive nature and intensity of the Casimir force at[4–15] or out of[16] thermal equilibrium, with potential technological applications to minimize stiction, friction or adhesion in nano and microscale devices[17–21]. Additionally, several works considering plane-parallel systems containing metallic[22–26], or ferromagnetic[27] materials as well as magneto-dielectric metamaterials[28] have also demonstrated that it is possible to alter the nature and intensity of the Casimir force by modifying the temperature. In the same context, theoretical predictions have shown that gravity and repulsive Casimir forces acting in plane-parallel dielectric structures can be fine-tuned and balanced at room temperature giving rise to levitation phenomena[29,30]. Temperature may affect the equilibrium position at which the dielectric films levitate in two ways: on the one hand, the contribution of thermal modes to the Casimir force at (and around) room temperature becomes significant when dielectric materials and separation distances > 100 nm are considered[31,32] (in contrast to metallic plates for which this contribution is assumed to be negligible). These thermal modes[2,33,34] are related to lengthscales $\lambda_T = \frac{\hbar c}{k_B T} \approx$ 7-8 μm at room temperature, with c the speed of light, T the temperature, and k_B and $\hbar$, the Boltzmann and the reduced Planck's constant, respectively. On the other hand, the density of the fluid mediating the interaction may be slightly altered with temperature, and so, the balance of Casimir, gravity, and buoyancy forces may occur at a different separation distance bringing the system into a new equilibrium state at the new temperature. Uncontrolled deviations of the equilibrium position of suspended films due to temperature variations may be detrimental for the proper operation of nano and micro-devices in which these films may be incorporated[35–38]. Therefore, a detailed analysis of the effect of temperature variations on the equilibrium position of suspended films in levitating plane-parallel configurations is desired.

Here, we analyze theoretically the effect of temperature variations on the equilibrium distance (d_{eq}) at which thin films levitate over a substrate due to the balance of Casimir ($\overrightarrow{F_C}$), gravity ($\overrightarrow{F_g}$), and buoyancy ($\overrightarrow{F_B}$) forces. We consider plane-parallel structures that have already been shown to display levitation at thermal equilibrium[30] that comprise dielectric materials, for which temperature effects are expected to be much larger than for metals[39]. In contrast to other approaches in which a system in horizontal arrangement is brought to a certain equilibrium position by an external harmonic-oscillator force acting on the system in addition to the Casimir force[39,40], in our setup thermal effects can be analyzed through the influence of gravity and buoyancy forces in vertical arrangement by evaluating the equilibrium distances at which thin dielectric films levitate over a substrate at different temperatures. In particular, we analyze free-standing thin films made of Teflon, silica (SiO_2), or polystyrene (PS), immersed in glycerol suspended over a silicon substrate, yielding short (< 100 nm) or large (> 600 nm) d_{eq} values depending on the selected material. Our choice of materials is not arbitrary: we consider dielectrics whose optical properties have been extensively studied in literature and do not change with temperature, that are chemically stable when combined together, that can be easily implemented for experimental realization, and with den-

a) Electronic mail: sol.carretero@csic.es
b) Electronic mail: h.miguez@csic.es

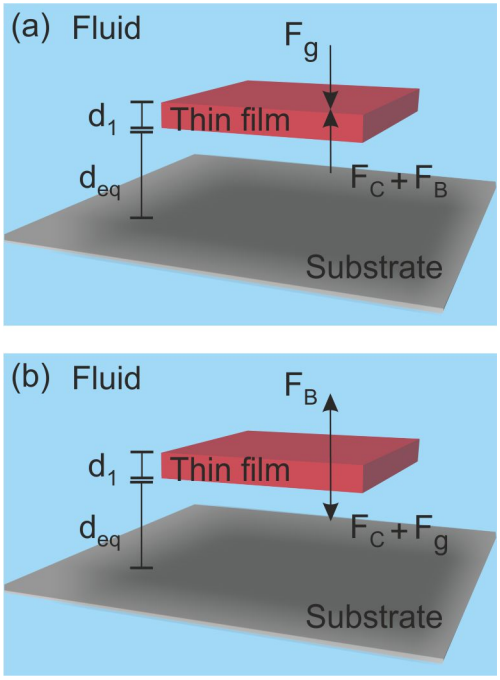

FIG. 1. Schematics of a plane-parallel system consisting on a thin film (of thickness d_1) fully immersed in a fluid standing over a semi-infinite substrate. The balance of Casimir ($\overrightarrow{F_C}$), gravity ($\overrightarrow{F_g}$) and buoyancy ($\overrightarrow{F_B}$) forces acting on the system gives rise to levitation at a certain, stable (a) or unstable (b), equilibrium distance (d_{eq}).

sities such that gravity and buoyancy forces can balance the Casimir force at a given separation distance. We find that the stability nature of d_{eq} is preserved under temperature changes, and that the effect of temperature variations on the Casimir force, and thus on d_{eq}, is dominated by transverse-magnetic modes at zero frequency. We provide simple rules to predict whether the equilibrium position takes place closer or further from the substrate at the new temperature that depend on the static permittivity contrast of the materials involved, as well as on the stability nature of d_{eq}.

A schematic of the plane-parallel structure under study is shown in Fig. 1. It consists on a free-standing thin film (of thickness d_1) immersed in a fluid facing a semi-infinite substrate. The separation distance between the thin film and the substrate at which the total force ($\overrightarrow{F_T} = \overrightarrow{F_C} + \overrightarrow{F_g} + \overrightarrow{F_B}$) cancels, defines d_{eq}. The two possible scenarios of the forces acting on the system, which determine the stability nature of d_{eq}, are presented in panels (a) and (b). In panel (a) a repulsive Casimir force ($F_C > 0$) is acting on the planar arrangement and it dominates at short separation distances (d_0), providing stable d_{eq} when the total force is canceled. This means that any slight deviation from the equilibrium position will lead to forces pointing to that stable location. In panel (b) an attractive Casimir force ($F_C < 0$) dominating at short separation distances is contemplated, giving rise to unstable equilibrium positions that will cause that the film will float or sink if it deviates from d_{eq}.

II. THEORETICAL FORMALISM

In order to determine the equilibrium distance at which free-standing thin films immersed in a fluid levitate over a substrate, it is necessary to compute the total force acting on the system, and find the separation distance at which $\overrightarrow{F_T}(d_0 = d_{eq}) = 0$.

In our model, the plane-parallel system is represented as a multilayer structure in which each layer is made of a material m[32]. The material mediating the interaction, in this case a fluid, is denoted by $m = 0$. Positive and negative m values stand for materials above and below the fluid, correspondingly. Thus, $m = +1$, $m = +2$ and $m =$ -1 accounts for the free-standing film, the fluid over it, and the substrate, respectively. The thickness of each layer is indicated by d_m.

For gravity and buoyancy forces we take $\overrightarrow{F_g} + \overrightarrow{F_B} = (\rho_{film} - \rho_{fluid}) \cdot g \cdot d_1$, with $g = 9.81$ m/s^2, and ρ the density of either the film or the fluid. Please note that all forces are expressed per unit area.

The Casimir force in plane-parallel systems explicitly depends on d_0 and T, and it can be expressed as a sum of two components:

$$F_C(d_0,T) = \sum_{j=[TE,TM]} F_{C,j}^{n=0}(d_0,T) + \sum_{j=[TE,TM]} F_{C,j}^{n>0}(d_0,T) \tag{1}$$

where n describes the discrete and infinite Matsubara frequencies, $\xi_n = \frac{2\pi k_B T}{\hbar} \cdot n$ with $n = 0, 1, 2,...$ The two components defining the Casimir force account for zero frequency ($n = 0$) and positive frequency ($n > 0$) modes of the transverse magnetic ($j =$ TM) and transverse electric ($j =$ TE) fields, whose corresponding expressions are[32]:

$$F_{C,j}^{n=0}(d_0,T) = -\frac{k_B T}{2\pi} \int_0^\infty \boldsymbol{k}_\perp^2 \, d\boldsymbol{k}_\perp \left[\frac{e^{2k_\perp d_0}}{R_j^{(+)} \cdot R_j^{(-)}} - 1 \right]^{-1} \tag{2}$$

$$F_{C,j}^{n>0}(d_0,T) = -\frac{k_B T}{\pi} \sum_{n=1}^{\infty} \int_0^\infty k_n^{(0)} \boldsymbol{k}_\perp \, d\boldsymbol{k}_\perp \times \left[\frac{e^{2k_n^{(0)} d_0}}{R_j^{(+)} \cdot R_j^{(-)}} - 1 \right]^{-1} \tag{3}$$

Note the $\frac{1}{2}$ factor in Eq.(2). In the above equations, $k_n^{(0)}$ is the wavevector perpendicular to the plane of the surfaces of the fluid medium ($m = 0$), and $\mathbf{k}_\perp$ is in turn, the projection of the wave-vector over the plane perpendicular to $k_n^{(0)}$. The multiple Fresnel coefficients $R_j^{(\pm)}(n, \mathbf{k}_\perp)$

that express the reflectance on either the top (+) or the bottom (−) surface of the fluid, are expressed as:

$$R_j^{(\pm)}(n,\boldsymbol{k}_\perp) = \frac{r_j^{(0,\pm1)} + r_j^{(\pm1,\pm2)} e^{-2k_n^{(\pm1)} d_{\pm1}}}{1 + r_j^{(0,\pm1)} r_j^{(\pm1,\pm2)} e^{-2k_n^{(\pm1)} d_{\pm1}}} \tag{4}$$

with $r_j^{(m,m')}$ the simple Fresnel coefficients at the interface between materials m and m', and $k_n^{(m)}$ the wavevector in the corresponding layer. For TM and TE polarizations the corresponding $r_j^{(m,m')}$ definitions read:

$$r_{TM}^{(m,m')}(n,\boldsymbol{k}_\perp) = \frac{\varepsilon_n^{(m')} k_n^{(m)} - \varepsilon_n^{(m)} k_n^{(m')}}{\varepsilon_n^{(m')} k_n^{(m)} + \varepsilon_n^{(m)} k_n^{(m')}} \tag{5}$$

$$r_{TE}^{(m,m')}(n,\boldsymbol{k}_\perp) = \frac{\mu_n^{(m')} k_n^{(m)} - \mu_n^{(m)} k_n^{(m')}}{\mu_n^{(m')} k_n^{(m)} + \mu_n^{(m)} k_n^{(m')}} \tag{6}$$

where $\varepsilon_n^{(m)}$ and $\mu_n^{(m)}$ are the material permittivity and permeability, respectively, evaluated at Matsubara frequencies. The wavevector $k_n^{(m)}$ is defined as:

$$k_n^{(m)} = \left[\boldsymbol{k}_\perp^2 + \varepsilon_n^{(m)} \frac{\xi_n^2}{c^2}\right]^{1/2} \tag{7}$$

and the permittivity $\varepsilon_n^{(m)}$ takes the form:

$$\varepsilon_n^{(m)} \equiv \varepsilon(i\xi_n) = 1 + \frac{2}{\pi}\int_0^\infty \frac{\omega\varepsilon''(\omega)}{\omega^2 + \xi_n^2}\, d\omega \tag{8}$$

being $\varepsilon''(\omega)$ the imaginary part of the dielectric function of material m at ω frequencies, $\varepsilon = \varepsilon'(\omega) + i\varepsilon''(\omega)$.

Specifically, in our studies non-magnetic materials are considered, so $\mu_n^{(m)} = 1$[2,41]. In addition, as the dielectric slabs are assumed to be fully immersed in a fluid, $m = +2$ accounts for the same fluid as $m = 0$, so we can take $r_j(+1,+2) = -r_j(0,+1)$. Finally, both a semi-infinite fluid above the suspended thin film and silicon substrate are considered, i.e., $d_{+2}, d_{-1} \to \infty$, rendering the simplification of the multiple Fresnel coefficient of the bottom surface to $R_j^{(-)} = r_j^{(0,-1)}$. In our calculations, the density of the materials at room temperature takes the values: $\rho_{Teflon} = 2200$ kg/m^3, $\rho_{SiO_2} = 2650$ kg/m^3, $\rho_{PS} = 1050$ kg/m^3 and $\rho_{glycerol} = 1256$ kg/m^3. Although the density of glycerol, which is the medium mediating the interaction, varies with T and thus affects $\overrightarrow{F_B}$ when the temperature is modified, these variations might be assumed to be negligible as the density of glycerol within the temperature range here considered hardly changes 0.7 %. Therefore, despite the fact that in our calculations proper $\rho_{glycerol}$ values will be taken at each temperature, variations of d_{eq} with temperature will be mainly dictated by $\overrightarrow{F_C}$. In addition, in our calculations we have not taken into account the possible effect of Casimir-Polder interactions at intermolecular separations between glycerol molecules and solid interfaces, as their impact in the determined levitation distances is estimated to be minor.[42,43]

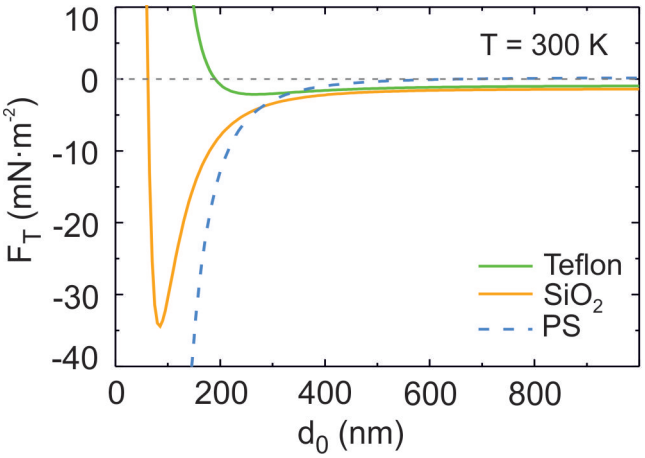

FIG. 2. Total force (per unit area) as a function of the separation distance (d_0) between a thin film of 100 nm thickness (d_1) made of Teflon, silica (SiO_2) or polystyrene (PS) (green, orange, and blue lines, correspondingly) immersed in glycerol facing a silicon substrate at 300 K of temperature (T). Values of d_{eq} are respectively: 190 nm, 60 nm and 667 nm. Solid and dashed lines stand for systems of stable or unstable equilibrium positions, respectively.

III. RESULTS AND DISCUSSION

Figure 2 shows the total force (per unit area) as a function of d_0 acting on a system comprising Teflon (green line), SiO_2 (orange line) or PS (blue line) slabs of d_1 = 100 nm, a thickness chosen according to feasible experimental realization, immersed in glycerol facing a silicon substrate. At room temperature (T = 300 K) and at thermal equilibrium, the predicted d_{eq} values are 190 nm, 60 nm, and 667 nm for the three materials, respectively. Stable d_{eq} positions are found for Teflon and SiO_2, whereas for PS films, d_{eq} is unstable. The different stability nature of the equilibrium positions attained are defined by the optical properties of the materials[30]. Taking these systems as reference, in what follows we will analyze the stability and variations of the equilibrium positions under temperature changes around room temperature.

Top panels in Fig. 3 show $\overrightarrow{F_T}$ acting on the same three planar systems analyzed in Fig. 2, as a function of d_0 and at several temperatures at thermal equilibrium. In all cases the trend of $\overrightarrow{F_T}$ with d_0 is preserved when temperature changes, attaining stable positions for Teflon and SiO_2 films, and unstable ones for PS slabs at thermal equilibrium. This means that for the plane-parallel arrangements here considered, the stability of the equilibrium position is not affected by temperature variations. Calculations of the Casimir force as a function of d_0 for

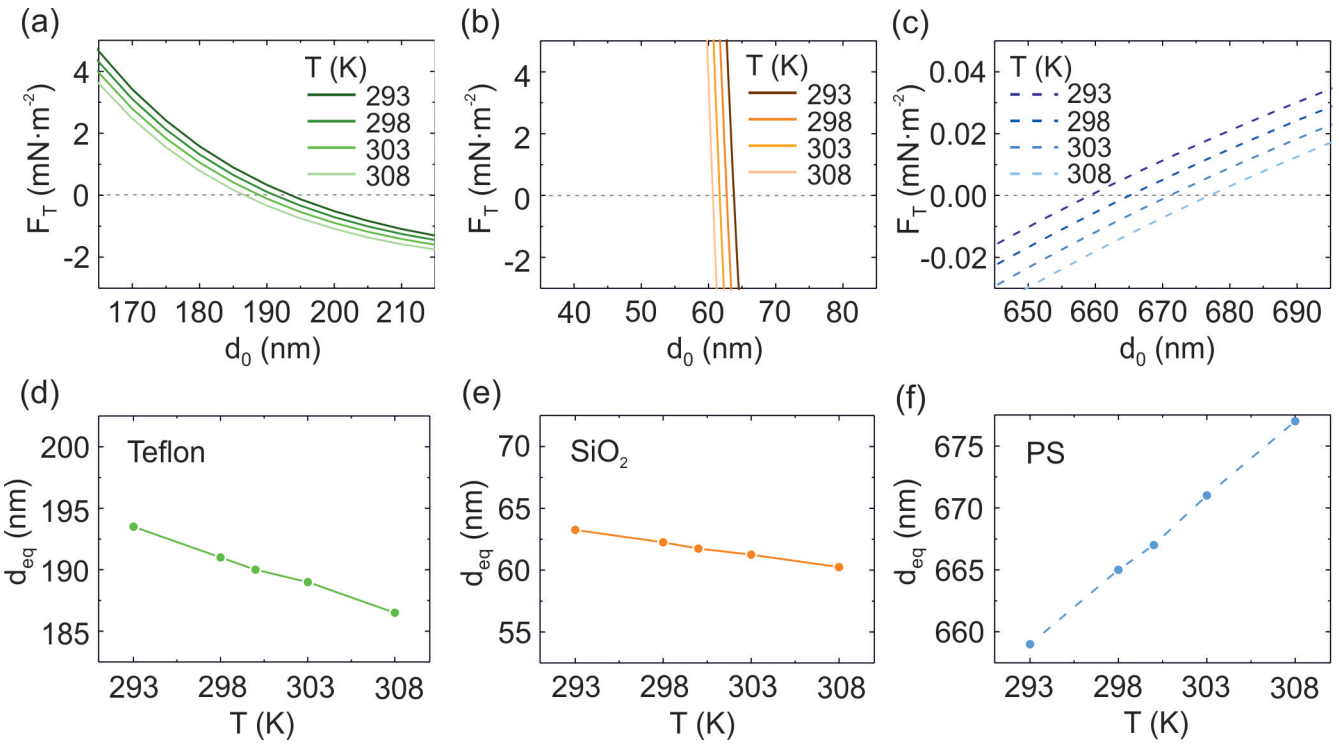

FIG. 3. (a),(b),(c) Total force (per unit area) as a function of the separation distance (d_0) between a thin film of 100 nm thickness (d_1) made of Teflon, SiO_2, or PS, respectively, immersed in glycerol facing a silicon substrate at different temperature around room temperature (T = 293, 298, 303, 308 K). At each temperature $\rho_{glycerol}$ takes the alues $\rho_{glycerol}$ = 1261, 1258, 1255 and 1252 kg/m^3. (d),(e),(f) Equilibrium distances obtained in corresponding top panel as a function of temperature. Solid and dashed lines stand for systems of stable or unstable equilibrium positions, respectively.

several temperatures are shown in Fig. S1 in the Supplemental Material[44]. In addition, we can see that in all cases the total force is altered with temperature variations. Specifically, as temperature rises 5 ^{o}C, equidistant curves are attained, shifting horizontally a constant increment. Note that the scale of $\overrightarrow{F_T}$ in Fig. 3(c) is 100 times smaller than in panels (a) and (b), therefore the variation of $\overrightarrow{F_T}$ with T for the PS system is much smaller than for structures incorporating Teflon or SiO_2 materials. Bottom panels in Fig. 3 display the collected equilibrium distances obtained in corresponding top panels at different temperatures. We find that in configurations containing Teflon and SiO_2 films d_{eq} decreases when T increases, with the smallest variations attained for SiO_2 films. PS films, in contrast, get away from the substrate as temperature rises, covering the largest d_{eq} range despite this system presents the smallest variations of $\overrightarrow{F_T}$ with T (Fig. 3(c)). Therefore, changes of d_{eq} with T are related not only to the temperature dependence of $\overrightarrow{F_T}$, but also to the variation of $\overrightarrow{F_T}$ with the separation distance near d_{eq}, and the stability nature of d_{eq}, which is provided by the trend of $\overrightarrow{F_T}$ as a function of d_0 that specifically depends on the optical properties of the materials considered[30].

To explain the approach or distance of the dielectric slabs to the substrate due to thermal effects, we first assume that the contribution of $\overrightarrow{F_B}$ to the variations of the total force with temperature can be neglected, since the density of glycerol hardly changes 0.7 % within the temperature range here considered. Therefore, we can accept that the main effect of temperature variations to the total force comes from the Casimir force, i.e., $\frac{\partial F_T}{\partial T} \approx \frac{\partial F_C}{\partial T}$. Secondly, we analyze the different $F^n_{C,j}$ contributions in Eqs. (2) and (3) defining the Casimir force under temperature changes. This kind of analysis has revealed that the $F^{n=0}_{C,TE}$ modes control the nature of the Casimir force in plane-parallel systems containing magnetic plates[4,6,8], or that the main contribution to $\overrightarrow{F_C}$ between graphene sheets comes from the $F^{n=0}_{C,TM}$ modes at room temperature[45].

To identify the effect of temperature changes in the $F^n_{C,j}$ contributions, the separation distance is fixed whereas temperature is varied around room temperature. As a representative structure showing large variations of $\overrightarrow{F_T}$ with T, we analyze a SiO_2 film of d_1 = 100 nm thickness suspended at d_0 = 60 nm at room temperature immersed on glycerol. Notice that in this specific case $d_0 = d_{eq}$, but it is not a necessary request for the analysis of the temperature dependence of the Casimir force here performed. Panel (a) in Figure 4 shows the $F^n_{C,j}$ contributions as a function of temperature. Full symbols denote zero-frequency modes (n = 0), and empty

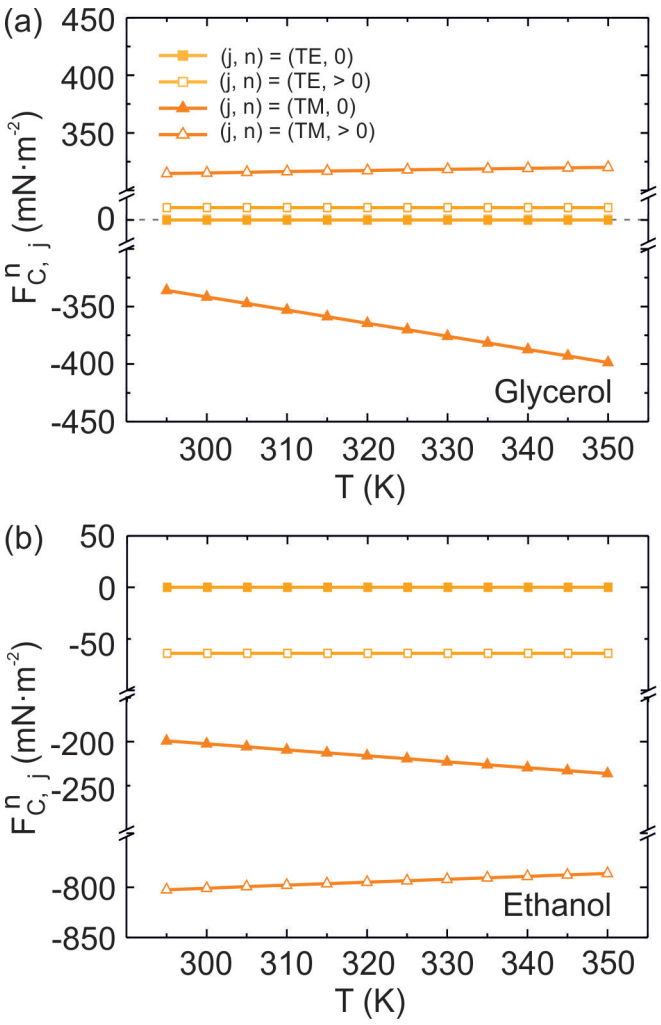

FIG. 4. $F^n_{C,j}$ contributions to the Casimir force as a function of temperature for a system consisting on a SiO_2 thin film of 100 nm, immersed in a fluid over a silicon substrate at d_0 = 60 nm for T = 300 K. Panel (a) corresponds to glycerol and panel (b) to ethanol as the mediating fluid. Transverse electric (TE) and transverse magnetic (TM) modes are displayed with square and triangle symbols, respectively. Zero frequency and non-zero frequency modes are shown with full and empty symbols, accordingly.

symbols positive frequencies ($n > 0$). Squares account for TE contributions, and triangles for TM ones. As expected $F^{n=0}_{C,TE} = 0$, as it has been assumed that $\mu^{(m)} = 1$ for all dielectric materials here considered, and so, Eq. (6) becomes zero. In addition, when all contributions are compared at a given temperature we observe that the largest contributions come from $F^{n=0}_{C,TM}$ modes, as it was the case of graphene sheets at room temperature[45]. Most importantly, in panel (a) the largest variations of $F^n_{C,j}$ with temperature are found for $F^{n=0}_{C,TM}$ contributions, while the other components remain almost unaltered, i.e., $\frac{\partial F^{n>0}_{C,TM}}{\partial T}, \frac{\partial F^{n>0}_{C,TE}}{\partial T}, \frac{\partial F^{n=0}_{C,TE}}{\partial T} \approx 0$. The same $F^{n=0}_{C,TM}$ dominance at finite temperature, and large variations of $F^{n=0}_{C,TM}$ with temperature are found for systems with Teflon or PS thin films embedded in glycerol, as it is shown in Fig. S2 in the Supplemental Material[44]. We also analyzed the same dielectric thin films immersed in ethanol or water instead of glycerol. Except for Teflon films in ethanol, the other sets of materials do not give rise to levitation. Panel (b) in Fig. 4 shows results attained for a silica film immersed in ethanol. We find that $F^{n=0}_{C,TM}$ modes are no longer the dominant ones, and instead, $F^{n>0}_{C,TM}$ provides the largest contribution to the Casimir force. In this case an attractive Casimir force together with gravity is always larger than the buoyancy force at all separation distances, preventing levitation. In these systems immersed in ethanol or water deprived of levitation, the $F^{n=0}_{C,TM}$ contribution also changes significantly with temperature. However, in some cases, the $F^{n>0}_{C,TM}$ component changes in such a way that it counteracts the $F^{n=0}_{C,TM}$ variations, that is, $\frac{\partial F^{n=0}_{C,TM}}{\partial T} \approx -\frac{\partial F^{n>0}_{C,TM}}{\partial T}$, impeding a simple prediction of the temperature effect in d_{eq} in those systems (results shown in Fig. S3, S4, and S5 in the Supplemental Material[44]). Therefore, in what follows, we will focus our analysis on the effect of temperature variations just in systems for which we can approximate:

$$\frac{\partial F_C}{\partial T} \approx \frac{\partial F^{n=0}_{C,TM}}{\partial T} \tag{9}$$

For TM polarization, Eq. (2) reads:

$$\begin{aligned} F^{n=0}_{C,TM} &= -T \cdot \frac{k_B}{2\pi} \int_0^\infty \boldsymbol{k}_\perp^2 \, d\boldsymbol{k}_\perp \left[\frac{e^{2|\boldsymbol{k}_\perp| d_0}}{R^{(+)}_{TM} \cdot R^{(-)}_{TM}} - 1 \right]^{-1} \\ &= -T \cdot \gamma \left(d_0, d_1, \varepsilon_0^{(m)} \right) \end{aligned} \tag{10}$$

in which the multiple ($R^{(\pm)}_{TM}$) and simple ($r^{(\pm)}_{TM}$) Fresnel coefficients for $n = 0$ take the form:

$$R^{(+)}_{TM} = \frac{r^{(0,+1)}_{TM} - r^{(0,+1)}_{TM} \cdot e^{-2\boldsymbol{k}_\perp d_1}}{1 - r^{2(0,+1)}_{TM} \cdot e^{-2\boldsymbol{k}_\perp d_1}} \tag{11}$$

$$R^{(-)}_{TM} = \frac{\varepsilon_0^{(-1)} - \varepsilon_0^{(0)}}{\varepsilon_0^{(-1)} + \varepsilon_0^{(0)}} \tag{12}$$

$$r^{(0,+1)}_{TM} = \frac{\varepsilon_0^{(+1)} - \varepsilon_0^{(0)}}{\varepsilon_0^{(+1)} + \varepsilon_0^{(0)}} \tag{13}$$

$$r^{(0,-1)}_{TM} = R^{(-)}_{TM} \tag{14}$$

Equation (10) reveals that $F_{C,TM}^{n=0}$ is linearly dependent on temperature and proportional to a function that defines the sensitivity of the Casimir force to temperature changes, $\gamma(d_0, d_1, \varepsilon_0^{(m)})$. This function accounts for the reach of the Casimir interaction through the separation distance (d_0) and the thickness of the thin film (d_1). It also depends on the optical properties of the materials, specifically, on the static permittivity of all objects in the system ($\varepsilon_0^{(m)}$). Figure S6 in the Supplemental Material[44] shows results of $\gamma(d_0, d_1, \varepsilon_0^{(m)})$ as a function of d_1, for different separation distances d_0 are shown for Teflon, SiO_2, and PS in. We find that the largest $\gamma(d_0, d_1, \varepsilon_0^{(m)})$ values are attained for very thin films of high dielectric contrast at short separation distances.

Next, in order to determine whether the new equilibrium position will take place closer or further from the substrate due to temperature variations, we first assume that the total force depends linearly with d_0 around d_{eq}, so for a given temperature T_1, we can write:

$$\mathrm{F}_T(d_0, T_1) \approx \tfrac{\partial F_T}{\partial d_0}|_{d_{eq}} \cdot d_0 + (d_0 - d_{eq}) \tag{15}$$

with $\frac{\partial F_T}{\partial d_0}$ the slope of the line. In addition, since parallel and equidistant curves are attained as temperature varies (top panels in Fig. 3), for a different temperature T_2 (with $T_2 > T_1$ or $T_2 < T_1$) we take

$$\mathrm{F}_T(d_0, T_2) \approx \tfrac{\partial F_T}{\partial d_0}|_{d_{eq}} \cdot d_0 + ((d_0 - d_{eq}) + \tfrac{\partial F_T}{\partial T}|_{d_{eq}} \cdot \Delta T) \tag{16}$$

We define $d_{eq}^{(1)}$ and $d_{eq}^{(2)}$ as the distances at which $\overrightarrow{F_T}(d_{eq}^{(1)}, T_1) = 0$ and $\overrightarrow{F_T}(d_{eq}^{(2)}, T_2) = 0$, correspondingly. Recalling that temperature variations of the total force can be approximated to be produced just by Casimir force variations, i.e., $\frac{\partial F_T}{\partial T} \approx \frac{\partial F_C}{\partial T}$, and that parallel curves have been attained, i.e., $\frac{\partial F_T}{\partial d_0}|_{d_{eq}^{(1)}} = \frac{\partial F_T}{\partial d_0}|_{d_{eq}^{(2)}}$, the variation of the equilibrium distance Δd_{eq} with temperature can be written as:

$$\Delta d_{eq} = d_{eq}^{(2)} - d_{eq}^{(1)} \approx -\frac{\left(\frac{\partial F_C}{\partial T}\right)|_{d_{eq}} \cdot \Delta T}{\left(\frac{\partial F_T}{\partial d_0}\right)|_{d_{eq}}} \tag{17}$$

Combining together Eqs.(9), (10), and (17), we have:

$$\begin{aligned}\Delta d_{eq} &\approx -\frac{\left(\frac{\partial F_C}{\partial T}\right)|_{d_{eq}} \cdot \Delta T}{\left(\frac{\partial F_T}{\partial d_0}\right)|_{d_{eq}}} \approx -\frac{\left(\frac{\partial F_{C,TM}^{n=0}}{\partial T}\right)|_{d_{eq}} \cdot \Delta T}{\left(\frac{\partial F_T}{\partial d_0}\right)|_{d_{eq}}} \\ &= \frac{\gamma(d_{eq}, d_1, \varepsilon_0^{(m)}) \cdot \Delta T}{\left(\frac{\partial F_T}{\partial d_0}\right)|_{d_{eq}}}\end{aligned} \tag{18}$$

In the above expression, the sign of $\gamma(d_{eq}, d_1, \varepsilon_0^{(m)})$ and $\frac{\partial F_T}{\partial d_0}$ (that defines the stability nature of d_{eq} at a given temperature), will determine whether the new equilibrium position will take place closer ($\Delta d_{eq} < 0$) or further ($\Delta d_{eq} > 0$) from the substrate with T variations. The sign of $\gamma(d_{eq}, d_1, \varepsilon_0^{(m)})$ is in turn defined by the denominator $R_{TM}^{(+)} \cdot R_{TM}^{(-)}$ in Eq. (10), since $\left|R_{TM}^{(\pm)}\right| < 1$, and the exponential is always > 1.

which relies upon the contrast between $\varepsilon_0^{(m)}$ of all materials involved in the levitating system (Eqs. (13) and (14)). For our systems, the fluid-slab interface is the only one modified while the fluid-substrate one is kept the same. Corresponding $\varepsilon_0^{(m)}$ values are: ε_0^{Teflon} = 2.1, $\varepsilon_0^{SiO_2}$ = 3.7, ε_0^{PS} = 2.45, $\varepsilon_0^{glycerol}$ = 42.4 and $\varepsilon_0^{silicon}$ = 11.74. In general, in a plane-parallel structure displaying levitation dominated by zero-frequency TM modes, if the static permittivities of all materials fulfill any of the following inequations: $\varepsilon_0^{(1)} > \varepsilon_0^{(0)} > \varepsilon_0^{(-1)}$ or $\varepsilon_0^{(1)} < \varepsilon_0^{(0)} < \varepsilon_0^{(-1)}$, the sign of the denominator is negative and therefore the sign of the $\gamma(d_{eq}, d_1, \varepsilon_0^{(m)})$ function. If d_{eq} is stable ($\frac{\partial F_T}{\partial d_0}|_{d_{eq}} < 0$) at a given temperature, $\Delta d_{eq} > 0$ as temperature rises, and so the system reaches the equilibrium position further away from the substrate. In the opposite case if d_{eq} is unstable ($\frac{\partial F_T}{\partial d_0}|_{d_{eq}} > 0$), the system will find the equilibrium state closer to the substrate. On the other hand, if the static permittivities of all materials in a plane-parallel system do not fulfill any of the above inequations, the sign of $\gamma(d_{eq}, d_1, \varepsilon_0^{(m)})$ function is positive and so d_{eq} will become shorter with T for stable equilibrium positions, or larger for unstable ones. These two scenarios correspond to Teflon and SiO_2 films in Fig. 3 (d) and (e), for which closer equilibrium positions are found as T rises, and PS thin films in Fig. 3 (f), where d_{eq} increases with temperature, accordingly. In Table I we gather and summarize all the possible $\varepsilon_0^{(m)}$ combinations, the stability of d_{eq}, and the prediction of Δd_{eq} with T. Note that for predicting the behavior of d_{eq} with T changes, all that needs to be known is the stability of d_{eq} at a given temperature, and $\varepsilon_0^{(m)}$ of all materials in the system. This analysis is only possible because in the systems under study the effect of temperature variations on the Casimir force is dominated by zero-frequency TM modes. Therefore, we could say that the effect of temperature variations on the equilibrium distance in systems displaying levitation rely on intrinsic properties of the materials comprising the system. This is of utmost importance, since some of the proposed routes to fine tune the Casimir force entail the design of the material optical properties of the system[14], by either modifying the dielectric function at certain frequency ranges while maintaining the static permittivity by means of photonic crystals[46], or by modifying the dielectric function including the static permittivity upon crystallization[47], for instance. According to our results, the use of photonic crystals operating in the UV-VIS-IR range would not have an influence on the equilibrium position under temperature variations, while the crystal-

$\varepsilon_0^{(1)} > \varepsilon_0^{(0)} > \varepsilon_0^{(-1)}$	$\varepsilon_0^{(1)} < \varepsilon_0^{(0)} < \varepsilon_0^{(-1)}$	d_{eq} Stability	$d_{eq}(T)$
yes	no	stable	increase
no	yes	stable	increase
yes	no	unstable	decrease
no	yes	unstable	decrease
no	no	stable	decrease
no	no	unstable	increase

TABLE I. Possible $\varepsilon_0^{(m)}$ relations of all materials comprised in a system that, together with the stability nature of d_{eq}, provide information of whether at the new temperature, the new equilibrium state occurs closer to (d_{eq} decreases) or further from (d_{eq} increases) the substrate. These results are valid only as long as the temperature dependence of the system is dominated by the $F_{C,TM}^{n=0}$ contribution.

lization approach would bring the suspended film to a different equilibrium state, as long as zero-frequency TM modes dominate the contribution to the Casimir force.

The quantification of the deviation from the equilibrium position of suspended films due to temperature variations depends on the interplay between $\gamma(d_{eq}, d_1, \varepsilon_0^{(m)})$ and $\frac{\partial F_T}{\partial d_0}$, and for this, the full calculation of $\frac{\partial F_T}{\partial d_0}$ is needed. In any case, an examination of Eq. (18) indicates that for systems with $\frac{\partial F_T}{\partial d_0} \to \infty$ slope, unmodified equilibrium distances are predicted ($\Delta d_{eq} \approx 0$), whereas in the opposite limiting case, for $\frac{\partial F_T}{\partial d_0} \to 0$, the equilibrium position of the levitating film will be strongly modified. These two limiting situations would correspond to SiO_2 films for which large values of $\frac{\partial F_T}{\partial d_0}$ are observed in Fig. 3 (b), and almost the same d_{eq} are obtained irrespective of the temperature considered (Fig. 3 (e)), whereas for PS films almost *zero* slope lines are found (Fig. 3 (c) and (f)) and so, the largest d_{eq} range is obtained.

IV. CONCLUSION

We have performed a theoretical analysis of the effect of temperature variations of suspended free-standing thin films in dielectric plane-parallel arrangements under the influence of Casimir, gravity and buoyancy forces at thermal equilibrium. In particular, thin films made up of Teflon, SiO_2, or PS immersed in glycerol facing a silicon substrate are considered. For all temperatures evaluated, we find that the trend of the total force acting on the system is kept as the separation distance varies, and so the stability nature of the equilibrium distances under temperature changes is preserved. In addition, the effect of temperature variations on the total force acting on the systems is dominated by the transverse-magnetic modes at zero-frequency defining the Casimir force which depends upon intrinsic dielectric properties of the system. We provide simple rules to predict whether the new equilibrium position takes place closer or further from the substrate in levitating arrangements at a different temperature, what can be inferred from the stability nature of the equilibrium state and the static permittivites of all materials comprising the system. Our results serve as a guide for designing planar arrangements in levitation mode to be incorporated in nano and micro-devices in which the equilibrium distance can be fine-tuned with temperature simply attending to the materials static permittivities contrast, or for observing the dynamic Casimir effect as the dielectric slab reaches the new equilibrium position at a different temperature.

ACKNOWLEDGMENTS

We acknowledge support from the European Research Council under the European Union's Seventh Framework Programme (FP7/2007-2013)/ERC grant agreement n^o 307081 (POLIGHT) and the Spanish Ministry of Economy and Competitiveness under grant MAT2014-54852-R. V. E. is grateful to "Obra Social La Caixa" for its support.

[1] H. B. G. Casimir, "On the attraction between two perfectly conducting plates," Proc. K. Ned. Akad. Wet. **51**, 793 (1948).
[2] E. M. Lifshitz, "The theory of molecular attractive forces between solids," Sov. Phys. JETP **2**, 73 (1956).
[3] I. E. Dzayloshinskii, E. M. Lifshitz, and L. P. Pitaevskii, "Van der waals forces in liquid films," Sov. Phys. JETP **37**, 161 (1960).
[4] T. H. Boyer, "Van der waals forces and zero-point energy for dielectric and permeable materials," Phys. Rev. A **9**, 2078–2084 (1974).
[5] O. Kenneth, I. Klich, A. Mann, and M. Revzen, "Repulsive casimir forces," Phys. Rev. Lett. **89**, 033001 (2002).
[6] N. Inui, "Temperature dependence of the casimir force between a superconductor and a magnetodielectric," Phys. Rev. A **86**, 022520 (2012).
[7] N. Inui, "Quantum levitation of a thin magnetodielectric plate on a metallic plate using the repulsive casimir force," J. Appl. Phys. **111**, 074304 (2012).
[8] N. Inui, "Thickness dependence of the casimir force between a magnetodielectric plate and a diamagnetic plate," Phys. Rev. A **84**, 052505 (2011).
[9] A. W. Rodriguez, A. P. McCauley, D. Woolf, F. Capasso, J. D. Joannopoulos, and S. G. Johnson, "Nontouching nanoparticle diclusters bound by repulsive and attractive casimir forces," Phys. Rev. Lett. **104**, 160402 (2010).
[10] J. N. Munday, F. Capasso, and V. A. Parsegian, "Measured long-range repulsive casimir-lifshitz forces," Nature **457**, 170 (2009).
[11] R. Zhao, J. Zhou, T. Koschny, E. N. Economou, and C. M. Soukoulis, "Repulsive casimir force in chiral metamaterials," Phys. Rev. Lett. **103**, 103602 (2009).
[12] P. J. van Zwol and G. Palasantzas, "Repulsive casimir forces between solid materials with high-refractive-index intervening liquids," Phys. Rev. A **81**, 062502 (2010).
[13] R. Zhao, T. Koschny, E. N. Economou, and C. M. Soukoulis, "Repulsive casimir forces with finite-thickness slabs," Phys. Rev. B **83**, 075108 (2011).
[14] L. M. Woods, D. A. R. Dalvit, A. Tkatchenko, P. Rodriguez-Lopez, A. W. Rodriguez, and R. Podgornik, *arXiv:1509.03338 [cond-mat.mtrl-sci]* (2015).
[15] J. C. Martinez and M. B. A. Jalil, "Tuning the casimir force via modification of interface properties of three-dimensional topological insulators," Journal of Applied Physics **113**, 204302 (2013).
[16] A. Noto, R. Messina, B. Guizal, and M. Antezza, "Casimir-lifshitz force out of thermal equilibrium between dielectric gratings," Phys. Rev. A **90**, 022120 (2014).

[17] F. M. Serry, D. Walliser, and G. J. Maclay, "The anharmonic casimir oscillator (aco) - the casimir effect in a model microelectromechanical system," J. Michroelectromech. Syst. **4**, 193–205 (1995).

[18] F. M. Serry, D. Walliser, and G. J. Maclay, "The role of the casimir effect in the static deflection and stiction of membrane strips in microelectromechanical systems (mems)," J. Appl. Phys. **84**, 2501–2506 (1998).

[19] J. Zou, Z. Marcet, A. W. Rodriguez, M. T. H. Reid, A. P. McCaulye, I. I. Kravchenko, T. Lu, Y. Bao, S. G. Johnson, and H. B. Chan, "Casimir forces on a silicon micromechanical chip," Nat. Commun. **4**, 1845 (2013).

[20] R. K. Zhao, A. Manjavacas, F. J. G. de Abajo, and J. B. Pendry, "Rotational quantum friction," Phys. Rev. Lett. **109** (2012).

[21] M. Sedighi and G. Palasantzas, "Influence of low optical frequencies on actuation dynamics of microelectromechanical systems via casimir forces," Journal of Applied Physics **117**, 144901 (2015).

[22] G. L. Klimchitskaya and V. M. Mostepanenko, Contemp. Phys. **47**, 131 (2006).

[23] I. Brevik, S. A. Ellingsen, and K. A. Milton, New J. Phys. **8**, 236 (2007).

[24] R. S. Decca, D. Lopez, E. Fischbach, G. L. Klimchitskaya, D. E. Krause, and V. M. Mostepanenko, Phys. Rev. D **75**, 077101 (2007).

[25] M. Boström and B. E. Sernelius, "Thermal effects on the casimir force in the $0.1^{\smile}$ $5\mu m$ range," Phys. Rev. Lett. **84**, 4757–4760 (2000).

[26] I. Brevik and J. S. Hoye, "Temperature dependence of the casimir force," Eur. J. Phys. **35**, 015012 (2014).

[27] B. Geyer, G. L. Klimchitskaya, and V. M. Mostepanenko, "Thermal casimir interaction betwen two magnetodielectric plates," Phys. Rev. B **81**, 104101 (2010).

[28] F. S. S. Rosa, D. A. R. Dalvit, and P. W. Milonni, "Casimir interactions for anisotropic magnetodielectric metamaterials," Phys. Rev. A **78**, 032117 (2008).

[29] M. Dou, F. Lou, M. Bostr´om, I. Brevik, and C. Persson, "Casimir quantum levitation tuned by means of material properties and geometries," Phys. Rev. B **89**, 201407 (2014).

[30] V. Esteso, S. Carretero-Palacios, and H. Míguez, "Nanolevitation phenomena in real plane-parallel systems due to the balance between casimir and gravity forces," J. Phys. Chem. C **119**, 5663–5670 (2015).

[31] G. L. Klimchitskaya and V. M. Mostepanenko, "Investigation of the temperature dependence of the casimir force between real metals," Phys. Rev. A **63**, 062108 (2001).

[32] M. Bordag, G. L. Klimchitskaya, U. Mohideen, and V. M. Mostepanenko, *Advances in the Casimir Effect*, 1st ed. (Oxford Science Publications, 2009).

[33] A. O. Sushkov, W. J. Kim, D. A. R. Dalvit, and S. K. Lamoreaux, "Observation of the thermal casimir force," Nature Physics **7** (2011).

[34] R. Guérout, J. Lussange, H. B. Chan, A. Lambrecht, and S. Reynaud, "Thermal casimir force between nanostrucutred surfaces," Phys. Rev. A **87**, 052514 (2013).

[35] H. B. Chan, V. A. Aksyuk, R. N. Kleiman, D. J. Bishop, and F. Capasso, "Quantum mechanical actuation of microelectromechanical systems by the casimir force," Science **291**, 1941 (2001).

[36] W. Broer, G. Palasantzas, J. Knoester, and V. B. Svetovoy, "Significance of the casimir force and surface roughness for actuation dynamics of mems," Phys. Rev. B **87**, 125413 (2013).

[37] Y. Fu, H. Du, W. Huang, S. Zhang, and M. Hu, "Tini-based thin films for mems applications," Sensors and Actuators A: Physical **112**, 395–408 (2004).

[38] S. Trolier-McKinstry and P. Muralt, "Thin film piezoelectrics for mems," Journal of Electroceramics **12**, 7–17 (2004).

[39] S. A. Ellingsen and I. Brevik, "Casimir force on real materialsthe slab and cavity geometry," J. Phys. A **40**, 3643 (2007).

[40] D. S. E. jr., L. B. Pires, S. Umrath, D. Martinez, Y. Ayala, B. Pontes, G. R. de S. Araújo, S. Frases, G.-L. Ingold, F. S. S. Rosa, N. B. Viana, H. M. Nussenzveig, and P. A. M. Neto, "Probing the casimir force with optical tweezers," EPL **112**, 44001 (2015).

[41] L. D. Landau, E. M. Lifshitz, and L. P. Pitaevskii, *Electrodynamics of Continuous Media*, 2nd ed. (Pergamon Press, 1982).

[42] M. Boström, S. Ellingsen, I. Brevik, D. F. Parsons, and B. E. Sernelius, "Sign of the casimir-polder interaction between atoms and oil-water interfaces: Subtle dependence on dielectric properties," Phys. Rev. A **85**, 064501 (2012).

[43] P. Thiyam, C. Persson, D. Parsons, D. Huang, S. Buhmann, and M. Boström, "Trends of co_2 adsorption on cellulose due to van der waals forces," Colloids Surf., A **470**, 316 – 321 (2015).

[44] See Supplemental Material at [URL will be inserted by publisher] for seeing the Casimir and total forces acting on the systems as a function of d_0, at different T; the different contributions to Casimir force in systems comprising thin films of Teflon, SiO_2 and PS immersed in glycerol, ethanol and water; and γ for all materials and different d_0 and d_1 values.

[45] G. L. Klimchitskaya and V. M. Mostepanenko, "Origin of large thermal effect in the casimir interaction between two graphene sheets," Phys. Rev. B **91**, 174501 (2015).

[46] R. Zeng and Y. Yang, "Repulsive and restoring casimir forces based on magneto-optical effect," Chin. Phys. Lett. **28**, 054201 (2011).

[47] G. Torricelli, P. J. van Zwol, O. Shpack, G. Palasantzas, V. B. Svetovoy, C. Binns, B. J. Kooi, P. Jost, and M. Wuttig, "Casimir force contrast between amorphous and crystalline phases of aist," Adv. Funct. Mater. **22**, 3729 (2012).